A LETTERS JOURNAL EXPLORING THE FRONTIERS OF PHYSICS

OFFPRINT

The effective Poisson ratio of random cellular matter having bending dominated architecture

A. BHASKAR

EPL, **87** (2009) 18004

TAKE A LOOK AT THE NEW EPL

Europhysics Letters (EPL) has a new online home at
www.epljournal.org

Take a look for the latest journal news and information on:

- reading the latest articles, free!
- receiving free e-mail alerts
- submitting your work to EPL

www.epljournal.org

A Letters Journal Exploring the Frontiers of Physics

July 2009

EPL, **87** (2009) 18004
doi: 10.1209/0295-5075/87/18004

www.epljournal.org

The effective Poisson ratio of random cellular matter having bending dominated architecture

A. Bhaskar[(a)]

Aeronautics & Astronautics, School of Engineering Sciences, University of Southampton - SO17 1BJ, Southampton, UK, EU

received 10 February 2009; accepted in final form 16 June 2009
published online 17 July 2009

PACS 81.05.Rm – Porous materials; granular materials
PACS 61.43.-j – Disordered solids
PACS 62.20.dj – Poisson's ratio

Abstract – We argue that the effective Poisson ratio of cellular and porous solids is independent of the material of the solid phase, if the mechanism of the cell wall deformation is dominated by beam bending —thus rendering it to be a purely kinematic quantity. Introducing a kinematic simplification and requiring statistical isotropy, we *prove* a result of remarkable generality that the effective Poisson ratio of irregular planar structures equals 1 for all bending dominated random architectures. We then explore a deeper connection of this behavior with area-preserving deformation of planar closed elastic cells. We show that thin sheets and films made of such microstructured material afford physical realizations of the two-dimensional analogue of incompressible matter. We term such non-stretchable sheet material as well as deformations as *isoektasic*.

Introduction. – Natural and synthetic porous materials such as bone, wood, metal foams [1], biological soft matter [2,3], and optical metamaterial have recently inspired many studies, relating structure to mechanical properties [4,5]. These studies include numerical [6] or laboratory experiments [7], analyses for regular lattices [8,9], the effect of non-homogeneity [10], or theoretical properties bounds [11,12]. Planar architectures are often called "honeycombs" whereas 3D structures are termed as solid "foams". We assume the cell walls to be made of homogeneous isotropic material, having Young's modulus E and Poisson's ratio ν. When remote stress is applied, the cell walls deform, resulting in bulk elastic response of the material which manifests as two effective elastic moduli $\bar{E}$ and $\bar{\nu}$. A majority of solids possess Poisson's ratio in the range 0.2 to 0.5, the theoretical limit for isotropic continuum being 0.5. Negative values of Poisson's ratio are not ruled out theoretically; however, physical realizations of negative Poisson's ratio material had to wait until the discovery of certain microstructural architectures that are usually attributed to "re-entrant corners" present in cells having non-convex shapes [13]. Such materials are also known as auxetic.

Complex cellular geometries such as those in fig. 1 are not amenable to exact analysis, experimentation can provide trends, and detailed computer analyses often obscure general understanding, despite being useful. In contrast, dimensional and scaling arguments are often simple, yet effective [14,15]. We express the effective Young modulus in the general functional form: $\bar{E} = f(E, \nu, \text{geometry})$. What role does the microstructural size have in determining the effective elastic properties and, for example, which of the three microstructures in fig. 1 will have the highest Young modulus? If the geometry of the microstructure is characterized by n parameters, the non-dimensional groups in this functional relationship are $\bar{E}/E$, ν, and $(n-1)$ non-dimensional parameters that describe the shape (*e.g.* the *ratios* of the length parameters or angles) because of

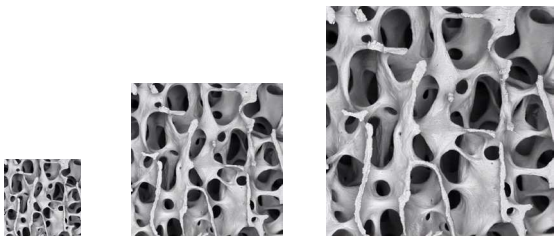

Fig. 1: A micrograph of bone uniformly expanded to three *different* hypothetical characteristic pore size (courtesy Alan Boyde, Queen Mary University, London).

(a)E-mail: A.Bhaskar@soton.ac.uk

Buckingham's Π-theorem [16]. Therefore, in terms of a new function Φ,

$$\bar{E} = E \times \Phi(\nu, \text{microstructural shape, topology}), \qquad (1)$$

where *shape* stands for the geometrical attributes that are invariant of scaling and *topology* stands for the nature of the connectivity. It now follows from eq. (1): *microstructural size has no role in determining the effective Young modulus*. We could come to this conclusion by formally expressing the quantities in terms of unknown powers and demanding dimensional homogeneity. The above conclusion is a mere reflection of the well-known fact that classical elasticity has no inherent length scale. The effective Poisson ratio, similarly, has the functional form $\bar{\nu} = g(E, \nu, \text{geometry})$. Dimensional homogeneity demands $\bar{\nu} \sim E^0$ which means that $\bar{\nu}$ does not depend on Young's modulus of the solid phase. We can similarly show that it does not depend on the microstructural size either, hence

$$\bar{\nu} = \Psi(\nu, \text{microstructural shape, topology}). \qquad (2)$$

That the effective moduli are scale invariant (*i.e.* they do not change on uniform expansion or contraction as in fig. 1) implies that, given microstructure, elastic properties are functions of the porosity (or the volume fraction) because porosity is scale invariant. Equations (1) and (2) are consistent with the detailed analysis for the special case of *thin walled regular hexagonal honeycombs* [8] because such lattices are geometrically similar for a given thickness–to–cell-wall-length ratio t/l. We have just shown that (1) and (2) are generally correct for all porous matter, simple or complex, such as those in fig. 1.

Turning to thin walled honeycombs, Torquato *et al.* [17] conjectured that *the effective moduli of any honeycomb structure in the low density limit are independent of Poisson's ratio of the solid phase* because the beam bending response depends on EI (the flexural stiffness) and the stretching response on EA (the axial stiffness) —both independent of ν; A is the cross-sectional area and I its second moment. However, this is invalid for honeycombs having thin but deep cell walls (*e.g.* for closed cell foams) because they behave as thin *plates* rather than thin *beams* even in the low density limit and because the plate bending rigidity, $D \sim (1-\nu^2)^{-1}$, depends on ν (admittedly a weak dependence for small ν but could be significant for material such as rubber, $\nu \approx 0.5$). On the other hand, the conjecture [17] is correct for open cell foams and filamentous planar networks because they possess beam-like thin cell walls. An immediate upshot of (2) is that the effective Poisson ratio of cellular solids governed by thin *beam strut* mechanics is a purely kinematic quantity: completely independent of the material of the cell walls!

The effective properties for several regular lattices as well as scaling arguments for random geometries have been clearly articulated in [4]. The effective Poisson ratio of a lattice of hexagonal beams has been calculated by Gibson *et al.* [4,7,8] who use detailed mechanics. In this approach, the response of the individual cell walls needs to be calculated first. This further enables one to calculate the bulk mechanical response in the directions along and perpendicular to the direction of the remote stress. The ratio of these two strain responses finally gives the effective Poisson ratio. While this works well with spatially periodic geometries such as the regular hexagonal honeycomb, it poses analytical difficulty with random networks because of the lack of a deterministic description of the latter. Our approach here, therefore, is statistical. Further, we restrict ourselves to planar networks.

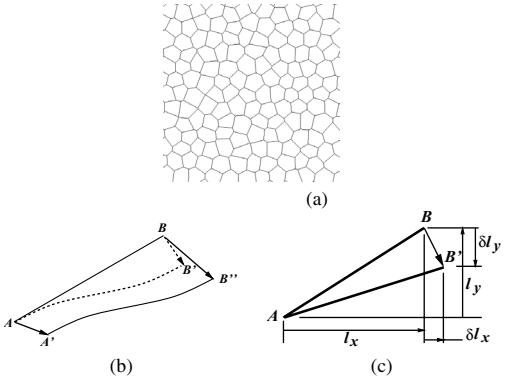

Fig. 2: (a) Part of a typical planar Voronoi structures analyzed, (b) a cell wall during flexure under remote horizontal stress, (c) the kinematic approximation of rigid-strut rotation.

A simplification of the network deformation kinematics and the effective Poisson ratio. – Consider *irregular* 2D networks such as the one shown in fig. 2(a) which was generated by using Voronoi construction for a set of random seed-points. The mechanism of deformation for kinematically rigid topologies is dominated by stretching —examples include topologies with triangular cells [18]. On the other hand, topologies such as the one shown in fig. 2(a) are kinematically mobile and they deform primarily in flexure. Consider a typical cell wall AB in fig. 2(b). When remote stress is applied horizontally, all the cell walls, in general, stretch and flex leading to displacement associated with each point of a cell wall. Ignoring the stretch deformation for the bending dominated architecture of fig. 2(a), the deflected shape is a cubic shape as shown by the solid line $A'B''$ because the governing equation of equilibrium is fourth order. The overall shape and size of the deformed bulk structure in 2(a) is determined by the positions of the cell wall joints. The change in the dimensions of the overall structure is related to the change in the projections of the cell walls along the horizontal and vertical directions. Now translate the deformed cell wall such that points A and A' coincide as shown using the curved dotted line in fig. 2(b). Because we are ignoring stretching deformation, $AB \approx AB'$. This simplifies the kinematics to the one shown in fig. 2(c) which shows a rigid strut in rotation and the resulting changes in the projections therefrom.

The horizontal and vertical projections of a typical cell wall AB of length l are l_x and l_y, respectively (fig. 2(c)). Under horizontal remote stress, these projections change by amounts δl_x and δl_y, respectively. The end point B assumes a new position B' when A and A' are made to coincide, as it would appear for an observer attached to point A. For stretch-free small deformation, vector BB' must be perpendicular to AB. The rotation of the cell walls manifests itself as elongation of the horizontal projection and a shortening of the transverse projection. Because changes in the projected lengths accumulate, they must lead to the changes in the overall horizontal and vertical lengths and are associated to the bulk strains in the two directions. When the cellular architecture is random, the average change in the projections along and across the the remote stress must be proportional to the original average projections in the respective directions. The constant of this proportionality equals the effective strains in the two directions, *i.e.*

$$\langle|\delta l_x|\rangle = \gamma_{\parallel} \langle|l_x|\rangle\,, \qquad \langle|\delta l_y|\rangle = -\gamma_{\perp} \langle|l_y|\rangle\,, \tag{3}$$

where the angular brackets mean average over the cell walls and the subscripts to the bulk strain γ refer to the directions with respect to remote loading. This statistical argument obviates detailed calculation of the response for a very large number of degrees of freedom which the rigid kinematics of cell walls alone cannot determine. For statistically isotropic networks,

$$\langle|l_x|\rangle = \langle|l_y|\rangle, \tag{4}$$

i.e. the total projections in any direction must be the same because such architectures must be free of directional bias. During inextensible deformation, $l_x^2 + l_y^2 = l^2$ is constant. Differentiating both sides, $l_x \delta l_x + l_y \delta l_y = 0$ which each cell wall must respect during the complex deformation of the network. Reorganizing terms and averaging over the cell walls after taking the absolute value of both sides, we have

$$\langle|\delta l_y|/|\delta l_x|\rangle = \langle|l_x|/|l_y|\rangle\,. \tag{5}$$

Since $|l_x|$ and $|l_y|$ are independent random variables, the mean of the quotient equals the quotient of the means. The changes in the projections $|\delta l_x|$ and $|\delta l_y|$ are also statistically independent (the ratio being a random variable defining the orientation of a cell wall). After using eqs. (3) and (4), we have

$$\bar{\nu} = -\gamma_{\perp}/\gamma_{\parallel} = \frac{\langle|\delta l_y|\rangle}{\langle|\delta l_x|\rangle} = \left\langle \frac{|\delta l_y|}{|\delta l_x|} \right\rangle. \tag{6}$$

Using eq. (5), demanding that $|l_x|$ and $|l_y|$ are statistically independent, and employing eq. (4) again, we obtain

$$\bar{\nu} = \left\langle \frac{|l_x|}{|l_y|} \right\rangle = \frac{\langle|l_x|\rangle}{\langle|l_y|\rangle} = 1. \tag{7}$$

This proves a remarkably general result that all statistically isotropic random planar elastic networks, having bending dominated architectures, have their effective Poisson ratio equal to 1. The importance of this result is highlighted by the fact that practically all known theoretical structure-property relationships are for lattice models [19]. Note that the result (7) excludes certain special architectures that have non-convex cells (eq. (3) does not hold in those cases; particularly the the sign of the second of the two) and they may show auxetic behavior [13,20,21]. Our theoretical result (7) is consistent with numerical observations and conjectures of Zhu *et al.* [6] and our own numerical experiments. To the best of our knowledge this general result has not been previously proven.

To verify the result (7) numerically, we generated Voronoi networks by creating edges from a set of randomly generated "seed-points" within a rectangular space. Voronoi cells guarantee convexity because they partition a plane into convex polygons. The randomness was achieved by randomizing the positions of the seed-points. However, the apparent randomness is restricted in that concave cells are excluded —a requirement for the validity of (3). Care was taken in ensuring that the cell density is fairly uniform despite randomness. If this is not done, the "sample size" required to ensure effective homogeneity at the bulk scale becomes very large. Each edge of the Voronoi network was modeled as an elastic beam strut having flexural as well as stretching degrees of freedom. The total elastic energy is expressed in terms of the degrees of freedom of the joints (2 translational and 1 rotational degrees of freedom per joint) and interpolating the stretching displacement linearly and the transverse deflection (associated with flexure) cubically. The potential energy of external remote stresses is calculated from the work done at the left and the right boundaries where stresses are applied. This term is a linear function of the generalized co-ordinates. Finally the principle of minimum total potential energy is applied and a set of linear algebraic equations of the form $\mathbf{Hq} = \mathbf{f}$ are variationally derived. Here $\mathbf{H}$ is the Hessian of the strain energy functional and $\mathbf{f}$ is the generalized force vector. In mechanics literature, this implementation is the well-known finite element method (the Hessian is also known as the stiffness matrix). These linear equations are solved for the unknown joint variables $\mathbf{q}$ and a complete displacement field is obtained.

A practical difficulty encountered with long and slender samples subjected to remote uniaxial stresses is that due to randomness, the structure is not perfectly symmetrical about the centreline of the sample, leading to an overall response in flexure transverse to the axis. This leads to significant curvature of the the bulk because the transverse response scales as $\sim(\mathrm{overalllength/overallthickness})^3$. Therefore, the aspect ratio of the samples was kept close to 1. To ensure that the length scale of heterogeneity (*i.e.* the characteristic cell wall length) is much smaller than the overall size of the sample, a large number of cells were included in each numerical experiment. Typically, each sample had over 1700 joints which corresponds to

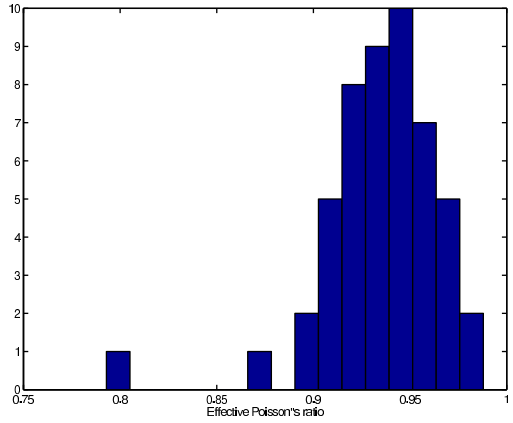

Fig. 3: (Colour on-line) A histogram of the computed effective Poisson ratio $\bar{\nu}$. Cell walls have bending and stretching flexibility.

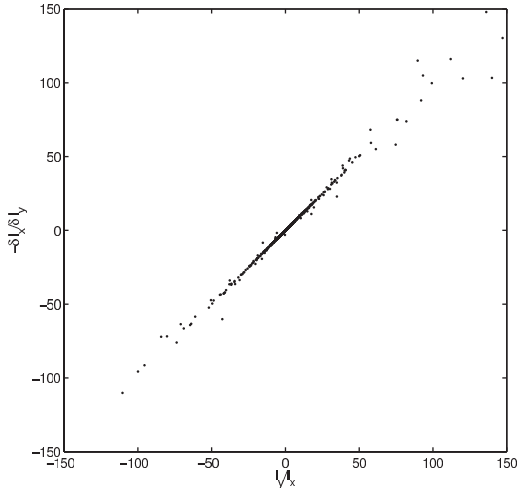

Fig. 4: $(-\delta l_x/\delta l_y)$ as a function of l_y/l_x for a typical numerical experiment. Each point corresponds to one cell wall.

more than 5100 degrees of freedom. The joints on the left edge were constrained horizontally but they had the freedom to move transversely. The effective Poisson ratio was calculated as the ratio $\bar{\nu} = -\gamma_\perp/\gamma_\parallel$ where the strains along and transverse to the applied stress were calculated from the averaged response at the four edges and the overall dimensions of the rectangular sample. A histogram of $\bar{\nu}$ for 50 such numerical experiments is shown in fig. 3. The mean value of $\bar{\nu}$ is obtained ≈ 0.94 which is very close to the predicted value 1. The difference between the theoretically predicted value 1 and the numerically observed values can be attributed mainly to the extension of the cell walls during deformations which is completely neglected while obtaining the result (7). In addition, other practical factors such as the finiteness of the sample with respect to typical cell size may also have contributed to this slight discrepancy.

Since the proof of eq. (7) crucially depends on the rigid-rotation assumption, we test its validity in the numerical experiments by plotting $-\delta l_x/\delta l_y$ as a function of l_y/l_x (the slope of a cell wall) in fig. 4. The data for each cell wall are plotted by a dot. Data for a large majority of cell walls align along the line through the origin at 45° —thus confirming rigid rotation of the cell walls under remote stress.

It has been suggested [4] that hexagonal honeycombs $(\bar{\nu} = 1)$ behave as isotropic media because the elastic moduli are directionally independent and because they satisfy the isotropic relationship for the shear modulus $\bar{G} = \bar{E}/2(1+\bar{\nu})$. However, thermodynamics demands Poisson's ratio for isotropic media to be in the range $-1 < \bar{\nu} < 0.5$. That the effective Poisson ratio $\bar{\nu}$ equals 1 for hexagonal honeycombs [4], as well as for irregular honeycombs (this letter), is not inconsistent with thermodynamics because *honeycombs are not isotropic*: they are "isotropic" only in the plane (hence $\bar{\nu} > 0.5$ is acceptable). On the planes perpendicular to the honeycomb, the properties are very different, hence non-isotropic. A most interesting implication of the effective Poisson ratio $\bar{\nu} \to 1$ is the exceptionally high stiffness for elastic properties containing terms such as $(1-\bar{\nu}^2)^{-1}$, *e.g.* for bending rigidity of plates.

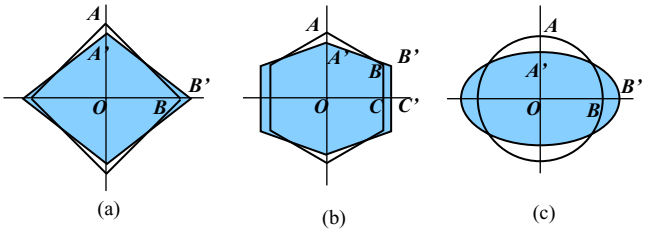

Fig. 5: (Colour on-line) (a) A cell (not in the sense of crystallographic unit cells) out of a square lattice of beams under remote horizontal stress. Triangles AOB and $A'OB'$ have the same area for small deflection. (b) A hexagonal cell: the quadrilaterals $AOCB$ and $A'OC'B'$ have equal area. (c) An isolated inextensible circular ring stretched horizontally. Deformed shapes are shaded in all the three cases.

***Isoektasic* deformation and non-stretchability of sheets and films.** – For the two-dimensional case under *uniaxial* remote tension, we can relate the fractional change in area to the strains by using the scaling argument. Consider a sheet of characteristic dimensions $L_x \times L_y$ thin in the z-direction and loaded parallel to the x-direction. After ignoring second order terms, we have $(\delta A/A) = \gamma_\parallel + \gamma_\perp$. Combining this with $\gamma_\perp = -\bar{\nu}\gamma_\parallel$, we have $(\delta A/A) = (1-\bar{\nu})\gamma_\parallel$. Therefore, $\bar{\nu}$ relates to the strain normalized fractional change in area as

$$\bar{\nu} = 1 - (\delta A/A)/\gamma_\parallel. \tag{8}$$

Now consider cells out of regular geometries *e.g.* the square honeycomb and the hexagonal honeycomb. A typical cell (not in the crystallographic sense) for the square lattice is shown in fig. 5(a). For simplicity, assume the sides of this square to be of unit length. When remote stress is applied horizontally, due to symmetry of

the loading and geometry, the deformed shape continues to have mirror symmetry about the horizontal and the vertical axes of the square. As a result, the four corner must fall on a rhombus after deformation. Ignoring the details of the complex shape of the four edges of the cell (which requires detailed mechanics), if $BB' = \mathrm{d}x$ which gives $AA' = \mathrm{d}x + O(\mathrm{d}x^2)$, the area of the rhombus spanned by the four corners is given by $1 + O(\mathrm{d}x^2)$. Hence, the change in area is an order higher than the order of strains. In the limit of small strains, therefore, the area remains unchanged. Similarly, using elementary geometry, the change in area for hexagonal cells (fig. 5(b)) can be shown to be zero (since four times the area of the rectangle $BB'C'C$ is compensated by the lost area of the two chevron shapes at the top and the bottom of the hexagon in fig. 5(b)) when a lattice containing such cells is stressed horizontally.

Symmetry and simple kinematics as presented above show that the net change in area $\delta A = 0$ for small strain *for each cell* in figs. 5(a) and (b). This implies that the change in area of the two-dimensional sheet made out of such cells must also remain unchanged upon uniaxial tension. Hence from equation (8), $\bar{\nu} = 1$! This agrees with the detailed calculation of [4] for the hexagonal honeycombs. Kinematic models have been qualitatively suggested in the past [13] mainly to explain auxetic behavior of regular lattices, often without recognizing that the fundamental assumption is the inextensibility of cell walls. We have just shown here that Poisson's ratio, as obtained kinematically here, is indeed *quantitatively exact*.

There appears to be a deeper connection between the inextensibility of the cell walls and area-preserving deformation of closed cells that extend roughly equally in the two directions in a plane. By "extending equally" we mean that the average inclinations of the cell walls and the resulting cell shape do not have any directional bias. It is hard to be precise about this for regular lattices, however, for random networks, the meaning can be made exact via appropriate shape measures or overall projections in two orthogonal directions (as is the case in this letter; eq. (4)).

It can be shown elegantly that an isolated thin inextensible circular ring, when loaded diametrically, deforms into an oval shape in such a way as to leave the area unchanged. Consider such a thin ring loaded by equal and opposite diametrical forces of magnitude F as shown in fig. 2(c). Due to the deformation of the ring, a displacement field associated with each point on the ring is given by $\mathbf{u}^F$ (the superscript denotes the actual problem of a ring loaded by discrete forces F). Now consider a hypothetical problem when the ring is loaded by an internal "pressure" p which acts radially outwards. Associated with this loading is a displacement field $\mathbf{u}^p$ which must be radial due to symmetry. If the radial displacement due to the pressure loading is δ^p, then the principle of reciprocity requires

$$F\delta^p = \oint p\mathbf{n}\cdot\mathbf{u}^F\,\mathrm{d}S, \tag{9}$$

where $\mathbf{n}$ is the outward drawn normal at the boundary of the circle. Because the ring is inextensible, there can be no radial displacement due to internal pressure, so $\delta^p = 0$ which means $\oint \mathbf{n}\cdot\mathbf{u}^F\,\mathrm{d}S = 0$ —thus the change in area due to diametrical force F must be zero. Hence the circle and the ellipse in fig. 5(c) have the same area. Although circles do not fit together to form a lattice and fill the plane, at the heart of Poisson's ratio being equal to 1 is this area preserving deformation of cells.

We now develop an expression for the change in area of a 2D solid of finite extent and of arbitrary shape under plane stress when traction is applied at the edges such that the resultant forces and moments of the applied traction are zero. The reciprocal theorem in elasticity can be expressed in terms of surface integrals

$$\int_{\partial V} n_i\sigma_{ij}^A u_j^B\,\mathrm{d}A = \int_{\partial V} n_i\sigma_{ij}^B u_j^A\,\mathrm{d}A \tag{10}$$

in the absence of body forces where the superscripts A and B are two different equilibrium states and σ_{ij} are the stress tensor components. Choose state A as the actual displacement, stress, and strain in the solid and state B as a hypothetical state of the same 2D body under hydrostatic edge tension (constant in value and normal to the local tangent). A guessed stress field $\sigma_{xx}^B = \sigma_{yy}^B = 1$, $\sigma_{xy}^B = 0$, (more compactly $\sigma_{ij}^B = \delta_{ij}$; where δ_{ij} is the Kronecker delta) is a valid equilibrium state for problem B because it can be shown to satisfy the plane stress equilibrium equations and the corresponding compatibility relation. The strain field is then given by $\gamma_{ij}^B = \frac{1-\bar{\nu}}{E}\delta_{ij}$ where the indices take values 1 and 2. Integrating the strain-displacement relationship $\gamma_{ij} = (u_{i,j} + u_{j,i})/2$ (the subscript following the comma means differentiation with respect to the corresponding spatial variable), we obtain the in-plane displacement field

$$u_i^B = \frac{1-\bar{\nu}}{E}x_i + c_i + \epsilon_{ij3}x_j\omega_3, \tag{11}$$

where c_i are the two arbitrary in-plane infinitesimal displacements, ω_3 is the infinitesimal rotation about an axis perpendicular to the plane of the solid, ϵ_{ij3} is the Levi-Civita permutation symbol with the third index fixed as 3, and summation over repeated indices is implicit. The three terms in eq. (11) represent dilatation without shape change, rigid-body translation, and rigid-body rotation, respectively. The change in area due to edge traction $t_j = \sigma_{ij}n_i$ is given by the contour integral $\delta A = \oint_C n_i u_i^A\mathrm{d}S$ which can be expressed as

$$\delta A = \oint_C n_i u_i^A\mathrm{d}S = \oint_C n_i\delta_{ij}u_j^A\mathrm{d}S = \oint_C n_i\sigma_{ij}^A u_j^B\,\mathrm{d}S \tag{12}$$

after specializing the reciprocity relation (10) for the plane stress problem. On account of translational equilibrium of the externally applied traction, the integral $\oint_C n_i\sigma_{ij}^A c_j\mathrm{d}S = 0$, and similarly, $\oint_C n_i\sigma_{ij}^A\epsilon_{jk3}x_k\omega_3\mathrm{d}S = 0$ for rotational equilibrium. The change in area due to

arbitrary traction $\mathbf{t}$ is then given by

$$\delta A = \frac{1-\bar{\nu}}{E} \oint_C x_i t_i \mathrm{d}S. \tag{13}$$

Note the strong similarity of this expression with the well-known result in elasticity for the change in volume of an isotropic solid $\delta V = \frac{1-2\nu}{E} \int_{\partial V} x_i t_i \mathrm{d}A$ subjected to surface traction. Apart from the surface integral instead of a contour integral, the main difference between this and (13) is the dependence on Poisson's ratio. The factor $(1-2\nu)$ for the expression of volume change is replaced by the factor $(1-\bar{\nu})$ for the expression of area change for the plane stress problems.

The $(1-2\nu)$-dependence of fractional volume change is consistent with the scaling argument. If the characteristic dimensions of a solid, slender in the x-direction, are $L_x \times L_y \times L_z$, then the fractional change in volume $\delta V/V = \delta L_x/L_x + \delta L_y/L_y + \delta L_z/L_z = (1-2\nu)\gamma_{\|}$ when loaded along the x-direction. Compare this with the fractional area change of a lamina given by $\delta A/A = (1-\nu)\gamma_{\|}$ (eq. (8)). Equation (13) shows a) that the $(1-\bar{\nu})$-dependence is not limited to simple geometries such at rectangular lamina; and b) it is true for any arbitrary traction, not just uniaxial tension.

From eq. (13), it follows that for all plane stress problems, the area preserving deformation (or coining a term, *isoektasic* —"ektasi" meaning area or extent) is associated with the effective in-plane Poisson ratio $\bar{\nu}$ being equal to 1. This is a two-dimensional analogue of the case of $\nu = 0.5$ for 3D solids (*i.e* associated with *isochoric* deformation) Since homogeneous isotropic materials cannot exceed a value of Poisson's ratio 0.5, 2D sheet/film of such material cannot exhibit isoektasic behavior. In fact, thin sheets of incompressible material ($\nu = 0.5$) will show an extension in area given by $\delta A/A = \gamma_{\|}/2$ when stretched remotely, according to eq. (8). Here, in microstructured material such as that in fig. 2(a), we have found a physical realization of "two-dimensional incompressibility", or "non-stretchability". The hexagonal lattice of beams then becomes the only known area preserving in-plane isotropic material having *regular* microstructure.

Conclusions. – We have shown using statistical arguments that cellular solids having random architectures of convex cells such as those in Voronoi networks must have in-plane Poisson's ratio equal to 1 when the dominant mechanism of cell wall deformation is flexure. Interestingly this value of Poisson's ratio coincides with Poisson's ratio for regular hexagonal lattice of beams. The basis of our proof is the statistical isotropy of random networks and a kinematic simplification that results from cell wall inextensibility. The simplified kinematics is found to be consistent with our numerical calculations. The numerically observed value of Poisson's ratio is slightly less than the theoretically predicted value 1. This difference is attributed to small stretch contribution to the cell wall deformation. We then show that thin sheets and films made out of such microstructured material will exhibit an area preserving property for any arbitrary geometry as long as the bulk matter is acted upon by traction at the edges that is in equilibrium. This behavior is a realization of the 2D analogue of isochoric deformation (associated with volumetric incompressibility). Accordingly, we propose to call such materials as isoektasic.

* * *

I thank my colleagues Professor N. Stephen, Dr P. Nair and Professor T. Sluckin for useful discussions; Professor A. Boyde of Queen Mary University, London for the micrograph in fig. 1.

REFERENCES

[1] Ashby M. F., Evans A. G., Fleck N. A., Gibson L. J., Hutchinson J. W. and Wadley H. N. G., *Metal Foams: A Design Guide* (Butterworth-Heinemann, Stoneham, Mass.) 2000.
[2] Warner M. and Edwards S. F., *Europhys. Lett.*, **5** (1988) 623.
[3] Warner M., Theil B. L. and Donald A. M., *Proc. Natl. Acad. Sci. U.S.A.*, **97** (2000) 1370.
[4] Gibson L. J. and Ashby M. F., *Cellular Solids: Structure and Properties,* 2nd edition (Cambridge University Press) 1997.
[5] Ashby M. F., *Philos. Trans. R. Soc.*, **364** (2006) 15.
[6] Zhu H. X., Hobdell J. R. and Windle A. H., *J. Mech. Phys. Solids*, **49** (2001) 857.
[7] Gibson L. J., PhD Thesis, Cambridge University Engineering Department, Cambridge (1981).
[8] Gibson L. J., Ashby M. F., Schajer G. S. and Robertson C. I., *Proc. R. Soc. London, Ser. A*, **382** (1982) 25.
[9] Deshpande V. S., Fleck N. A. and Ashby M. F., *J. Mech. Phys. Solids*, **49** (2001) 1747.
[10] Prakash O., Bichebois P., Louchet F. and Embury J. D., *Philos. Mag.*, **73** (1996) 739.
[11] Hashin Z. and Shtrikman S., *J. Mech. Phys. Solids*, **11** (1963) 127.
[12] Torquato S., *Appl. Mech. Rev.*, **44** (1991) 37.
[13] Lakes R. S., *Science*, **235** (1987) 1038; *Nature*, **414** (2001) 503.
[14] Barenblatt G. I., *Scaling, Self-similarity, and Intermediate Asymptotics* (Cambridge University Press) 1996.
[15] Taylor G. I., *Proc. R. Soc. London, Ser. A*, **201** (1950) 159.
[16] Buckingham E., *Phys. Rev.*, **4** (1914) 345; *Nature*, **96** (1915) 396.
[17] Torquato S., Gibiansky L. V., Silva M. J. and Gibson L. J., *Int. J. Mech. Sci.*, **40** (1998) 71.
[18] Deshpande V. S., Ashby M. F. and Fleck N. A., *Acta Mater.*, **49** (2001) 1035.
[19] Roberts A. P. and Garboczi E. J., *Acta Mater.*, **49** (2001) 189.
[20] Wojciechowski K. W. and Branka A. C., *Phys. Rev. A*, **40** (1989) 7222.
[21] Gasper N., Ren X. J., Smith C. W., Grima J. N. and Evans K. E., *Acta Mater.*, **53** (2005) 2439.